energies

MDPI

Article

Long-Term Performance of Thermal Insulating Composite Systems Based on Water Resistance and Surface Multifunctionality

Giovanni Borsoi [1,2], João L. Parracha [1,2], Jéssica D. Bersch [1], Ana R. Garcia [3,4], Amélia Dionísio [5], Paulina Faria [6], Rosário Veiga [2] and Inês Flores-Colen [1,*]

1 Civil Engineering Research and Innovation for Sustainability (CERIS), Department of Civil Engineering, Architecture and Environment (DECivil), Instituto Superior Técnico, University of Lisbon, Av. Rovisco Pais, 1049-001 Lisbon, Portugal; giovanni.borsoi@gmail.com (G.B.); jparracha@lnec.pt (J.L.P.); jessica.d.bersch@tecnico.ulisboa.pt (J.D.B.)
2 National Laboratory for Civil Engineering (LNEC), Av. do Brasil, 101, 1700-066 Lisbon, Portugal; rveiga@lnec.pt
3 Centro de Química Estrutural, Instituto Superior Técnico, University of Lisbon, Av. Rovisco Pais, 1049-001 Lisbon, Portugal; argarcia@ualg.pt
4 Department of Chemistry and Pharmacy, Faculty of Science and Technology, University of Algarve, Campus de Gambelas, 8005-139 Faro, Portugal
5 Centro de Recursos Naturais e Ambiente (CERENA), Departamento de Engenharia de Recursos Minerais e Energéticos (DER), Instituto Superior Técnico, University of Lisbon, Av. Rovisco Pais, 1049-001 Lisbon, Portugal; amelia.dionisio@tecnico.ulisboa.pt
6 Civil Engineering Research and Innovation for Sustainability (CERIS), Department of Civil Engineering (DECivil), NOVA School of Science and Technology, NOVA University Lisbon, 2829-516 Caparica, Portugal; paulina.faria@fct.unl.pt
* Correspondence: ines.flores.colen@tecnico.ulisboa.pt

Abstract

External Thermal Insulation Composite Systems (ETICSs) are increasingly applied in both new construction and energy retrofitting, where long-term durability under environmental exposure is critical to preserving thermal efficiency. Moisture ingress represents a key degradation factor, reducing insulation performance and undermining energy savings promoted by the ETICS. The effectiveness of these systems is strongly influenced by surface protection, which also reflects aesthetic and biological resistance. This study investigates the influence of three commercial protective surface coatings, characterized by hydrophobicity, photocatalytic activity, and resistance to biological growth, on ETICS finishes based on acrylic, natural hydraulic lime (NHL), and silicate binders. An artificial aging protocol was employed to evaluate coating stability and compatibility with the finishing layers. Results show that acrylic-based finishes provided superior durability and protection, while coatings on NHL and silicate substrates exhibited lower performance. Notably, a TiO_2 enriched photocatalytic coating, despite improved self-cleaning potential, demonstrated the least durability. The findings highlight that optimal ETICS protection requires coatings that combine low water absorption, effective drying, and biological resistance, thereby ensuring sustained thermal and energy performance over time.

Keywords: ETICS; multifunctional coatings; durability; hydrophobicity; self-cleaning; biocidal

Academic Editors: Umberto Berardi and Rafik Belarbi

Received: 1 August 2025
Revised: 31 August 2025
Accepted: 17 September 2025
Published: 20 September 2025

Citation: Borsoi, G.; Parracha, J.L.; Bersch, J.D.; Garcia, A.R.; Dionísio, A.; Faria, P.; Veiga, R.; Flores-Colen, I. Long-Term Performance of Thermal Insulating Composite Systems Based on Water Resistance and Surface Multifunctionality. *Energies* **2025**, *18*, 5008. https://doi.org/10.3390/en18185008

1. Introduction

External Thermal Insulation Composite Systems (ETICSs), also known as Exterior Insulation Finishing Systems (EIFSs) or Exterior Wall Insulation Systems (EWIs), consist of thermal insulation materials, such as expanded polystyrene (EPS), mineral wool (MW), or insulation cork board (ICB), bonded and/or mechanically fixed to façades and coated with a reinforced rendering (a base coat with a glass fiber mesh) and a finishing coat (e.g., paint) [1–3]. Since the 1960s, ETICSs have been widely used worldwide for new constructions and retrofitting [4] due to their contributions to thermal insulation, building envelope protection [5], and reductions in energy consumption and CO_2 emissions [6].

However, ETICSs are continuously exposed to environmental and anthropogenic agents [7] that affect their durability and in-service life, including wind-driven rain, solar radiation, atmospheric pollutants, and biocolonization [8–11]. Water accumulation or condensation can lead to several anomalies, including aesthetic changes and runoff stains, thermo-mechanical stresses and microcracks [12,13], biological growth (e.g., algae, fungi, bacteria, lichens) [14,15], and increased thermal conductivity of the insulation layer and the whole system [6].

Applying protective products to ETICS surfaces can help reduce degradation and enhance their durability. Multifunctional coatings and paints, which encompass biocide, hydrophobic, and self-cleaning properties, can provide a suitable maintenance strategy [16]. Nevertheless, the coexistence of these functions raises concerns about the materials' long-term performance and the suitability of their protection function.

Hydrophobic binders or additives (e.g., siloxane, silicates, silane, aliphatic or fluorinated compounds) provide a water-repellent barrier on façades, preventing the penetration of water and harmful ions (e.g., chlorides or sulfates) [17] and thus preserving the thermal resistance of ETICSs. Silicon-based water repellents can form covalent bonds with the substrate, resulting in a barrier at the air-substrate interface and/or nanoscale roughness [18]. These features induce low surface energy and increase the water contact angle. However, a lack of data on the durability of hydrophobic emulsion coatings is often reported in the literature [19,20].

Biocide additives in infinitesimal percentages (e.g., terbutryn, isothiazole, zinc pyrithione) within surface protective coatings can hinder biological growth [15]. Biocidal action generally includes enzymatic inactivation (disturbance of selected metabolic or energetic processes by disintegration or chemical modification of antimicrobial agents), reduced intracellular accumulation, specific reactions, and physicochemical alterations at the cellular target sites (i.e., mutational changes, chemical modification, and protection) [21].

Photocatalytic additives (e.g., titanium or zinc oxides, cadmium sulfide) provide self-cleaning, air-purifying, and antimicrobial properties [22] when applied to façades. Photocatalysts, activated by UV irradiation, accelerate photoinduced reactions and lead to a heterogeneous advanced oxidation process (formation of free radicals) [23,24], decomposing organic molecules and forming superhydrophilic surfaces that can facilitate the removal of contaminants [16,23,25–30].

A competitive effect between hydrophobic (water contact angle (θ) > 90° between drops and the surface due to water-repellent additives) and superhydrophilic properties (with $\theta \sim 0°$, induced by the photocatalytic products) can lead to a lack of long-term effectiveness [25,26]. Similarly, the durability of biocides is a significant concern for façades [31]. Although their use has been increasingly limited [32], leaching phenomena and degradation byproducts are rarely reported [33,34].

Most previous studies have addressed hydrophobic coatings, biocidal treatments, and photocatalytic additives independently. Comprehensive data on their combined long-term performance after aging remain limited [35–37]. In particular, the potential interactions

between these functionalities when applied to commercial ETICS [38] should be further clarified. Addressing this gap is essential not only for developing sustainable maintenance strategies for façades but also for advancing the scientific understanding of multifunctional coatings in building envelopes.

Therefore, this paper aims to investigate the performance of three commercially available multifunctional coatings with biocidal, hydrophobic, and photocatalytic properties when applied to four different widely used commercial ETICS. Their long-term efficacy was assessed by correlating moisture transport properties, mold growth, and photocatalytic activity to identify synergistic or competitive effects among the different additives. Additionally, incompatibilities between additives and some of the coatings were found. A recently developed innovative accelerated aging procedure [13], involving hygrothermal cycles, ultraviolet (UV) radiation, and exposure to air pollutants (SO_2), was conducted, including examining the chemical and morphological changes that occurred during aging.

2. Materials and Methods

2.1. Materials

2.1.1. ETICS

Four commercially available ETICSs, with a European Technical Approval (ETA), were selected based on the most common systems available on the market. The products feature various thermal insulation materials (including EPS, ICB, and MW), base coats (formulated with cement or natural hydraulic lime (NHL)), and finishing coats (acrylic-, lime-, or silicate-based), as shown in Table 1.

Table 1. Constituent layers and thicknesses of the studied ETICSs.

System Acronym	Thermal Insulation	Base Coat (BC) [1]	Finishing Coat (FC)		Thickness (mm)
			Key-Coat	Finishing	
S1	EPS	Cement, synthetic resins, mineral additives	Water-based acrylic dispersion	Water-based acrylic co-polymer, pigments, marble powder, and additives	40.6
S2	ICB	NHL, cement, mineral fillers, resins, and synthetic fibers	Air lime, hydraulic binder, and organic additives		65.8
S3	MW	Cement, synthetic resins, mineral fillers, and additives	Water-based acrylic co-polymer and mineral additives	Water-based acrylic paint, mineral aggregates, pigments, and additives	61.3
S4	ICB	NHL, cement, mixed binders, and cork aggregates	Water-based dispersion of silicate	Water-based silicate paint, organic additives, and pigments	43.9

[1] BC includes a reinforcement glass fiber mesh.

2.1.2. Multifunctional Coatings

Three commercial multifunctional coatings (MC) (Table 2) were applied to the dry surface of ETICS in two successive layers using a brush, following the manufacturers' guidelines. A 24 h interval was maintained between applications to allow for complete solvent evaporation. The coated ETICS specimens were stored under controlled conditions (T = 20 ± 3 °C, RH = 50 ± 5%) for three weeks to ensure complete polymerization of the coatings.

Table 2. Technical data for the multifunctional coatings (MCs), as reported in the manufacturers' technical and safety sheets.

Product Identification	Color	Density (g/cm^3) at T = 20 °C/ RH% = 60	pH	Drying Residue (g/L)	Application Yield (L/m^2)	Flash Point (°C)
HW	Whitish	0.99 ± 0.02	9.3 ± 0.5	59 ± 6	0.166–0.25 (no dilution)	64
NS	Whitish	0.98 ± 0.05	9.2 ± 0.5	30 ± 2	0.1–0.125 (no dilution)	>23
AQ	Transparent (opal)	1.31 ± 0.09	8.5 ± 0.5	718 ± 21	0.26–0.27 (10% dilution in water)	>100

According to the technical documentation, HW consists of an aqueous silane/siloxane emulsion with hydrophobic performance and biocidal additives (isothiazole). NS is an ethyl silicate-based coating with reduced percentages of silane, incorporating nanostructured TiO_2 particles that enable photocatalytic self-cleaning and antimicrobial properties. AQ is a multifunctional coating with hydrophobic, self-cleaning, and biocidal properties based on an acrylic aqueous dispersion (methyl methacrylate and butyl acrylate), also containing nano- to microstructured TiO_2 particles (10%), $CaCO_3$ (5 to 10%), quartz, ZnO, and biocidal additives (terbutryn, isothiazole).

2.2. Methods

2.2.1. Moisture Transport Properties

Capillary water absorption was tested according to EAD 040083-00-0404 [3]. Two specimens (with dimensions 150 mm × 150 mm × thickness, Table 1) of each "ETICS + MC" were used. The specimens were conditioned in a controlled environment (T = 23 ± 2 °C, RH = 65 ± 5%) for seven days before testing, and their lateral faces were sealed with metallic adhesive tape. The external surface of the specimens was placed in contact with water at approximately a 3 mm depth, and weight was recorded at selected intervals (i.e., after 3 min, 1, 2, 4, 8, and 24 h).

The capillary water absorption coefficient (Cc) was determined from the initial linear portion of the absorption curve, obtained by plotting the mass of absorbed water per unit area in contact with the water, kg/m^2, against the square root of time, min$^{0.5}$ [7]. Specifically, Cc was calculated as the slope of the absorption curve during the first 3 min of testing, by dividing the absorbed water mass per specimen area at 3 min by the square root of the time at this point. In addition, the mean water absorption of the specimens after 1 h and 24 h was considered for comparative purposes [3].

Drying kinetics were evaluated immediately after the capillarity test, following EN 16322 [39]. Weight loss was monitored until stabilization (defined as mass variation < 1%), under the same controlled environment (T = 23 ± 2 °C, RH = 65 ± 5%) [7]. The drying index (DI) was calculated with Equation (1), which describes the cumulative extent of water release during drying relative to the maximum possible water content and theoretical drying potential over time. In Equation (1), M_x is the mass of the specimen measured during the drying process (g), M_1 is the mass of the oven-dried specimen (g), M_3 the initial mass at the beginning of drying (g), t_0 (h) the initial test time and t_f (h) the ending time of

the drying process [40]. A lower *DI* value indicates faster water release and drying kinetics. For comparison, the same t_f was adopted for all samples.

$$DI = \frac{\int_{t_0}^{t_f} f\left(\frac{M_x - M_1}{M_1}\right) dt}{\left(\frac{M_3 - M_1}{M_1}\right) \times t_f} \quad (1)$$

2.2.2. Photocatalytic Efficacy and Color Change

Rhodamine B (RhB), functionalized diethylammonium chloride, $C_{28}H_{31}ClN_2O_3$) was selected for the photocatalytic assessment of the multifunctional coatings over time. A 0.05 g/l RhB water-based solution was prepared and applied with a micropipette to the specimen surface (80 mm × 45 mm × Thickness, Table 1), producing stains of approximately 2 cm in diameter [41]. Three stained specimens per set of "ETICS + MC" system were exposed in a UV-light chamber with three lamps (60 W/m^2, λ = 315–400 nm, UV-A), placed 5 cm away from the samples.

Color coordinates (L^*, a^*, and b^* from the CIELab color space) were measured using a Chroma Meter Minolta CR-410 chromameter (Konica Minolta, Inc., Tokyo, Japan). L^* indicates lightness (0 = black, 100 = white), a^* represents the red ($+a^*$) to green ($-a^*$) axis, and b^* the yellow ($+b^*$) to blue ($-b^*$) [16,42]. The equipment operated in specular component included mode (SCI) with D_{65} illuminant, 2° observer angle, and a 50 mm measurement area. Measurements were collected immediately after RhB application and after 4, 8, 24, 48, 72, 96, and 168 h of UV exposure.

Color change (ΔE, dimensionless) was calculated with Equation (2) [43], which expresses the overall difference in color between two measurements in the CIELab color space. In Equation (2), ΔL^*, Δa^*, and Δb^* are the mean differences in the corresponding coordinates (lightness L*, red-green a*, and yellow-blue b*, dimensionless) between the RhB-stained specimens at a time of interest (t) and their initial stained state at the beginning of the test (t = 0) [15,43,44]. A higher ΔE value indicates a more pronounced magnitude of color change.

$$\Delta E = \sqrt{(\Delta L^*)^2 + (\Delta a^*)^2 + (\Delta b^*)^2} \quad (2)$$

Color variations and/or preservation were further assessed by comparing the CIELab coordinates of unstained specimens before and after accelerated aging cycles. For this purpose, three specimens of each setting were studied, and six measurements were collected from each specimen.

2.2.3. Biological Colonization

The susceptibility to mold growth was examined on both unaged multifunctional coatings (tested alone) and "ETICS + MC" settings after completing the accelerated aging procedure (hygrothermal cycles, UV radiation, and SO_2 exposure, Section 2.2.4). A method adapted and previously validated for ETICS [7] was used in the analysis.

Unaged coatings (HW, NS, and AQ) were applied in three layers to both sides of Whatman three n° 1 filter paper (45 mm diameter), in accordance with the technical data sheets (see Table 2). Furthermore, three coated ETICS specimens of each system (50 mm × 50 mm × 20 mm) were tested after the complete aging procedure.

All specimens were steam-sterilized in an autoclave for 20 min, then placed on test flasks containing culture media (4% malt, 2% agar). A mixed aqueous spore suspension (2 mL) of *Aspergillus niger* and *Penicillium funiculosum* was evenly spread across the specimens and surrounding medium. The test flasks were placed for four weeks in a culturing chamber (T = 22 ± 1 °C, RH = 70 ± 5 %) [13]. A control group (three Whatman n° 1 filter papers and three *Pinus pinaster* wood samples) was included for validation [45].

Mold development was visually assessed weekly using the ASTM D5590-17 [46] rating scale: 0 for no apparent growth (0% of contaminated surface); 1 for traces of growth (<10% of contaminated surface); 2 for light growth (10–30% of contaminated surface); 3 for moderate growth (30–60% of contaminated surface); 4 for heavy growth (>60% of contaminated surface). After four weeks, specimens were removed, and the percentage of contaminated surface was confirmed under an Olympus B061 stereo microscope.

2.2.4. Accelerated Aging Procedure

Accelerated aging involved sequential exposure of "ETICS + MC" to hygrothermal cycles (HT), UV radiation (UV), and air pollutants (SO_2) [13,47]. After each type of exposure, all tests described in Sections 2.2.1–2.2.3 were performed, except for absorption and drying after SO_2 exposure (due to the reduced specimen size).

Hygrothermal aging was conducted following EAD 040083-00-0404 [3] in a FitoClima 10,000 ELC climatic chamber (Aralab, Rio de Mouro, Portugal). The insulation and basecoat layers (150 mm × 150 mm × Thickness—Table 1) were previously sealed with metallic tape and a sealing adhesive. Specimens were exposed to sprinklers with a water flux of 1 L/(m^2·min) and thermal IR lamps (8 × 250 W). 80 heat/rain cycles were carried out (for a total of 320 h), alternating 3 h at T = 70 ± 5 °C and RH = 10–30%, and 1 h of continuous water spray at T = 15 ± 5 °C. Specimens were left to drain for 2 h and then conditioned for 48 h at room temperature (T = 20 ± 5 °C, RH ≥ 50%). After this, five heat/cold cycles were performed (totaling 120 h): 8 h at T = 50 ± 5 °C and RH ≤ 30%, followed by 16 h at T = −20 ± 5 °C.

ISO 16474-3 [48] was followed for UV cycles, using a Q-Panel UV-light chamber. Specimens were exposed to 125 cycles (totaling 1000 h) of alternating 4 h of UV-A radiation (λ = 315–400 nm, 60 W/m^2) at T = 60 °C and 4 h of moisture at T = 50 °C, RH = 80%.

Air pollutant cycles were conducted in a FitoClima 300EDTU climatic chamber (Aralab). Specimens were in an SO_2-rich environment of 25 ppm (3% dilution in 3000 ppm of nitrogen). A total of 60 cycles (720 h) were carried out, alternating 6 h at T = 40 °C and RH = 30%, with 6 h at T = 15 °C and RH = 85% [13].

2.2.5. DRIFT and SEM-EDS Analyses

Diffuse Reflectance Infrared Fourier Transform (DRIFT) spectroscopy was performed to detect possible physical-chemical alterations and/or degradation in coated and uncoated ETICS surfaces. Measurements were conducted using a Bruker VERTEX 70 spectrophotometer (Bruker Optics GmbH & Co. KG, Ettlingen, Germany), equipped with an MCT broadband detector (spectral range: 4000–500 cm^{-1}) and a resolution of 4 cm^{-1}. Each spectrum was obtained from 200 accumulated single-beam scans, which were divided by the KBr spectrum (FTIR grade, background), and then converted to Kubelka-Munk units. Baseline correction was performed in OPUS software (version OPUS 9.0). Deconvolution was carried out in the 1915–1100 cm^{-1} region to study adsorbed water and coating carbonation [13].

Morphological and microchemical analyses were carried out using a ThermoScientific Phenom ProX G6 scanning electron microscope (SEM) (Thermo Fisher Scientific Inc., Waltham, MA, USA), equipped with a CsB6 filament and a light elements energy-dispersive spectroscopy (EDS) detector. Specimens were previously placed on Al stubs with double-sided carbon tape and sputtered with an Au-Pd (80:20) film using a Quorum Technologies Q150T ES system (Quorum Technologies Ltd., Laughton, UK).

3. Results

3.1. Moisture Transport Properties

Figure 1 illustrates the capillary water absorption coefficients (Cc) for all settings studied along the aging cycles. The three multifunctional coatings reduced water absorption by capillarity in the acrylic-finished ETICS S1 with EPS insulation, and the system generally maintained these values after undergoing artificial aging cycles. The hygrothermal cycles induced even a higher Cc reduction with the application of the hydrophobic silane/siloxane emulsion HW and the acrylic-based AQ, possibly due to a reduction in the pore size distribution and thus in wettability [13]. Conversely, the UV cycles led to a slight Cc increase, which can be attributed to the UV activation of photocatalytic additives (and thus formation of surfaces with higher hydrophilicity) [49].

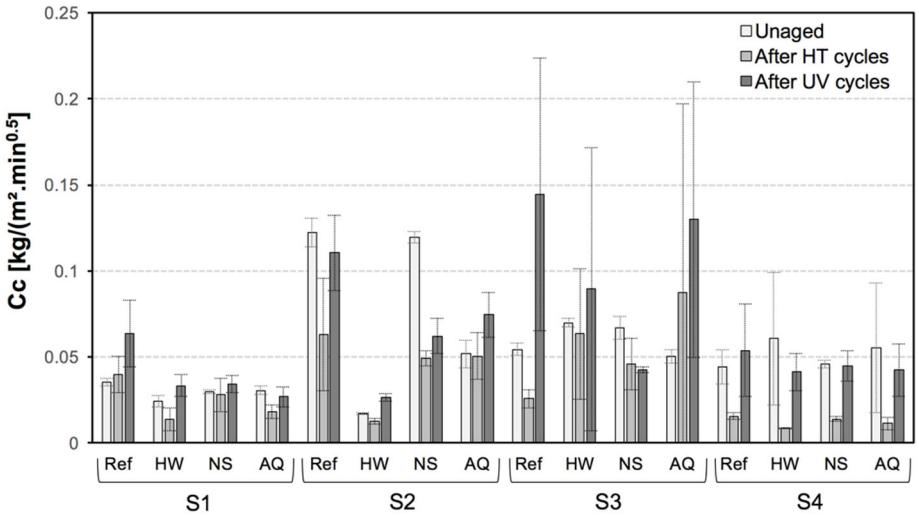

Figure 1. Average results and relative standard deviations for capillary water absorption coefficients (Cc) of the studied ETICS (S1–S4) without (Ref) and with protective treatments (HW, NS, and AQ), unaged and after hygrothermal (HT) and ultraviolet (UV) artificial aging cycles.

Concerning the NHL-based finished S2 ETICS with ICB insulation, which has noticeably higher water absorption compared to S1, the protective coatings reduced the Cc values. The application of the highly hydrophobic silane/siloxane emulsion (HW) induced the highest Cc reduction, in accordance with previous studies [20]. In contrast, slightly higher values were observed when the acrylic-based hydrophobic, self-cleaning, and biocidal AQ coating was applied. This latter product exhibited low wettability (Cc < 0.1 kg/(m^2·h)) after the aging cycles; however, its values are rather similar to those of the silicate-based NS, possibly due to the inclusion of hydrophilic nano- or micro-structured TiO_2 additives.

In the acrylic-finished ETICS S3 with MW insulation, no initial increase in Cc was observed with the application of protective coatings. The HT cycles had a moderate effect on the Cc values, whereas a significant rise in Cc was observed after the UV cycles. This variation can be attributed to the partial photodegradation of the acrylic-based surface and coatings during UV irradiation [50], which is associated with the use of a hydrophilic insulation layer (mineral wool). This layer can facilitate water absorption and retention, thereby reducing the effectiveness of protective products. The thermal conductivity is directly proportional to the water or moisture content [7].

The application of protective products did not significantly affect the Cc of the silicate-finished S4 system with ICB. The remarkable Cc reduction after hygrothermal cycles might indicate reduced compatibility and bonding among the silicate substrate and the waterborne products. Finally, an increase in water absorption is observed again after the UV cycles, due to the activation of the photocatalytic and thus hydrophilic additives.

Therefore, all the settings studied had a relevant reduction in Cc values after hygrothermal cycles. These data agree with previous works on hydrophobic treatments [20,51], which also identified lower Cc values after heat-cold and freeze–thaw cycles due to modifications in the pore size distribution of the substrates and/or physical-chemical alterations in the polymeric matrix of the multifunctional coatings. On the contrary, the UV cycles led to an increase in absorption in some cases, due to an increase in hydrophilicity and thus a decrease in the water contact angle [13,52–54].

Figure 2 shows the mean water absorption values of the studied settings after one hour. All unaged ETICS, with and without multifunctional coatings, met the requirement of EAD 040083-00-0404 [3], i.e., a water absorption of less than 1 kg/m^2 within one hour. However, S2-AQ considerably surpassed this threshold after hygrothermal cycles, as was also the case for S3-REF, S3-HW, and S3-AQ after hygrothermal and UV cycles. Conversely, the aged acrylic-finished S1 and silicate-finished S4 fulfilled the requirements in all conditions, with and without multifunctional coatings.

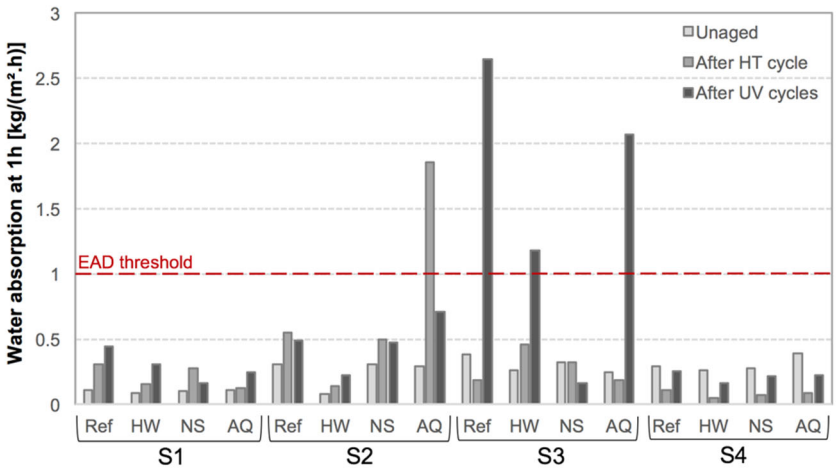

Figure 2. Mean water absorption at one hour of the studied ETICS S1–S4, without (Ref) or with protective treatments (HW, NS, AQ), unaged, and after HT and UV artificial aging cycles.

Figure 3 presents the drying index (DI) values obtained for the ETICS before and after the aging cycles. In the unaged state, it can be observed that the application of the hydrophobic, self-cleaning, and biocidal AQ coating induced the highest DI increase (i.e., slower drying rate), which is noticeable in the case of the NHL-finished S2 system.

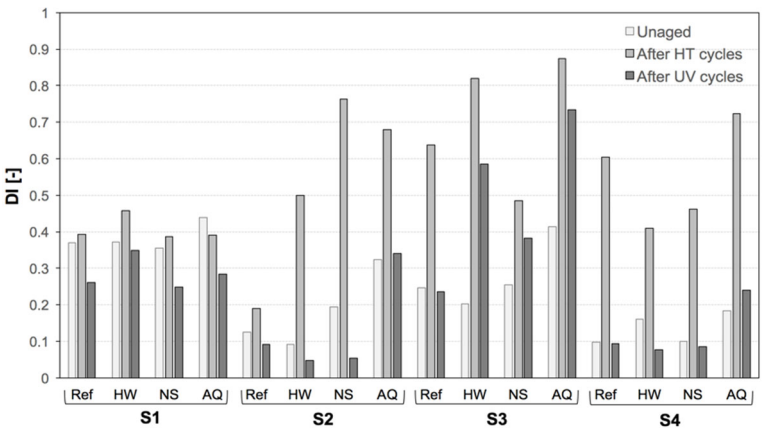

Figure 3. Average results for the drying index (DI) of the studied ETICS (S1–S4) without (Ref) and with protective coatings (HW, NS, AQ), unaged and after HT and UV aging cycles.

In contrast, HW and, more notably, the photocatalytic and antimicrobial coating NS caused minor changes, with values closer to those of the reference specimen. These data can be related to the significantly higher density and dry residual of the acrylic-based AQ product (Table 2), if compared to the silane-siloxane and ethyl silicate compositions of HW and NS, respectively. These data are in accordance with previous research [51], which indicated an increase in drying index results with acrylic-based hydrophobic products, characterized by low water vapor permeability, whereas siloxane-based products reduced the drying resistance.

Results showed that the hygrothermal cycles significantly affected the drying capacity of the products, with an increase in the DI values, especially when applied to ETICS S2, S3, and S4. This can indicate a relevant abrasion and alteration of the surface induced by the combined action of heat-cold and freeze–thaw cycles, affecting water loss in the liquid state (step I of drying) as well as water vapor permeability (step II of drying) [13,51].

On the other hand, a significant DI reduction (i.e., faster water evaporation) was observed after the UV cycles, with values closer to those of the unaged specimens. The NHL-finished S2 and silica-finished S4 systems with ICB insulation showed the lowest DI values, in accordance with previous studies [55]. Furthermore, the UV activation of photocatalytic additives (TiO_2) leads to hydrophilic properties, which can also enhance water vapor permeability and thus facilitate evaporation [16,56].

3.2. Color Change and Photocatalytic Efficacy

3.2.1. Chromatic Coordinates

The application of the NS and AQ products led to light whitening. In contrast, almost no chromatic variation (with a slightly glossier surface) was observed in the case of the hydrophobic/biocidal emulsion HW. When considering the color changes in the pristine specimens throughout the accelerated aging procedure (Figure 4), it can be observed that the NHL-finished ETICS S2 was the most chromatically affected (yellowish tone) after hygrothermal aging, both in the untreated specimens and the specimens with HW or NS. Conversely, the UV cycles induced a chromatic alteration not visible to the naked eye (i.e., $\Delta E < 2$) [57] in almost all specimens. In the case of aging cycles with SO_2, ΔE values were generally lower than 4 CIELab units, resulting in only a slight color variation.

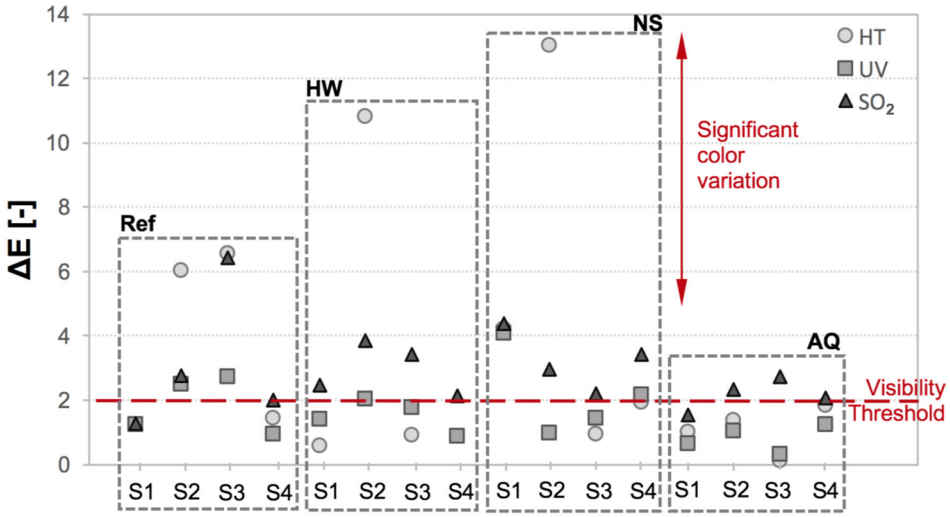

Figure 4. Average results for the color change (ΔE) of the studied ETICS S1–S4 without (Ref) and with protective coatings (HW, NS, AQ), after HT, UV, and SO_2 aging cycles.

No significant color variation was observed on the acrylic-finished ETICS (S1 with EPS and S3 with MW insulation) after aging, indicating proper chromatic compatibility of

the multifunctional protective coatings with these ETICS. NS and AQ provided the lowest chromatic alteration, possibly due to their photocatalytic properties, which may have contributed to maintaining the lightness and solar reflectance over time [49]. Indeed, TiO_2 nanoparticles possess unique amphiphilic (both hydrophilic and oleophilic) properties, which are based on their photocatalytic activation [16]. The photocatalytic properties led to a whitening of the surface, thereby contributing to maintaining the lightness and solar reflectance over time [49], and ensuring self-cleaning effectiveness, particularly in acrylic- (S1, S3) and silicate-finished (S4) ETICS.

It can be concluded that the NHL-finishing S2 system was the most chromatically affected by the aging cycles, while silicate-based finishing S4 ETICS presented the highest resistance, with or without multifunctional coatings. Hygrothermal cycles were the most invasive artificial aging process, particularly in the case of the protective products HW and NS, and with the untreated system S3.

3.2.2. Photocatalysis Evaluation

Regarding photocatalytic efficacy, Figure 5 illustrates the RhB decomposition (ΔE) over time for specimens along the aging protocol, compared to the initial values on RhB-dyed surfaces. In all cases, the color variation was significantly higher after 1 week of exposure to the UV-A lamp compared to a short-term (4 h) exposure. It is worth noting that 80% to 90% of the value obtained after one week (168 h) was achieved within 2 to 3 days of UV-A lamp exposure, confirming a relatively fast photocatalytic activity of the treatments.

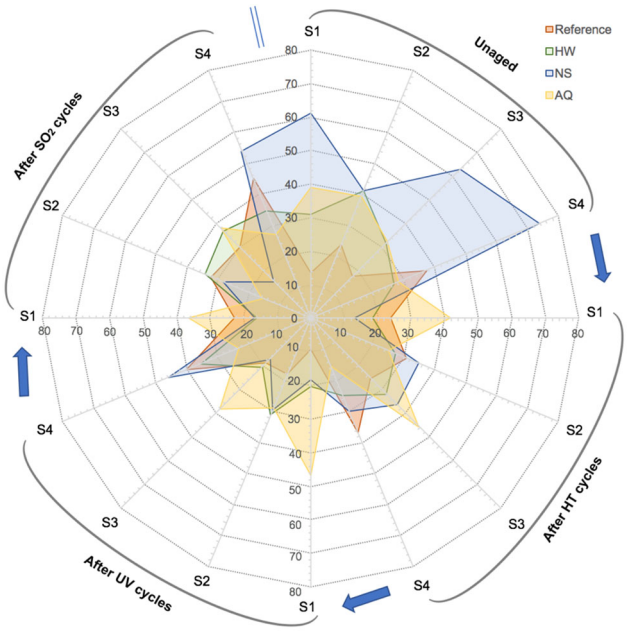

Figure 5. Average results for the color changes (ΔE), related to RhB decomposition after 168 h of UV-A lamp exposure of unaged and aged (after HT, UV, and SO_2 cycles) systems, with or without protective coatings.

Concerning the ETICS with no protective products, a significantly reduced self-cleaning capacity was observed in the acrylic-finished systems (S1 and S3), if compared to the NHL-finished (S2) and silicate-finished (S4) ICB ETICS. RhB also presents a dye-sensitized process, in addition to its degradation by TiO_2 particles under UV radiation [58]. The different aging cycles have a reduced effect on RhB degradation and, consequently, on the color change in the systems, confirming the relatively high resistance of the studied systems to aging (as observed in [13]).

In the unaged state, the most significant self-cleaning properties and, therefore, photocatalytic efficiencies were observed in the specimens treated with the photocatalytic and antimicrobial coating NS (Figure 5), due to the incorporation of TiO_2 nanoparticles with photoinduced properties [30]. The highest values were obtained for the ETICSs finished with acrylic and silicate products, rather than NHL. The application of AQ, which also presented considerable percentages of TiO_2 and ZnO, induced a higher photocatalytic effect in the acrylic- (S1, S3) and NHL-finished (S2) systems, if compared to the untreated specimens. Therefore, in the unaged state, an order NS > AQ > HW can be defined for self-cleaning effectiveness (Figure 5).

After artificial aging, the systems treated with NS showed a considerable reduction in ΔE after the hygrothermal cycles. Except for the silicate-finished S4 ETICS, the UV and SO_2 cycles resulted in even lower ΔE variations, thereby reducing photocatalytic activity and highlighting the reduced durability of NS to artificial aging. Acrylic-finished ETICS (S1 and S3) were generally more affected when compared to the inorganic finished (silicate or NHL) ETICS. It is worth noting that the association of wet and dry cycles, as well as prolonged exposure to UV radiation, can lead to partial removal of the protective product and/or the formation of micro-defects on the coating's surface [50]. Although TiO_2 nanoparticles are generally encapsulated (in e.g., SiO_2, Al_2O_3, or ZrO_2 as shell materials) to prevent the contact between the degradable organics and the photoactive TiO_2 surface, the photoinduced hydrophilicity and self-cleaning effectiveness of the treatment with nano-engineered TiO_2 can be partially reduced by weathering [44,59], with discoloration, loss of gloss, or chalking coatings.

The effect of the aging cycles was less significant in the case of the systems treated with HW and AQ, exhibiting considerable resistance to hygrothermal cycles, UV radiation, and SO_2-rich cycles. In accordance with previous studies [20,51], silane/oligomeric siloxane presented lower modification of their properties after aging, when compared to SiO_2-TiO_2 nanostructured treatments. The treatments with AQ showed significant resistance, also due to its considerable thickness, if compared to the other treatments (Table 1).

3.3. Biological Colonization

The average results of mold development on the coatings after four weeks of incubation on the unaged multifunctional products showed traces of mold growth in all three types of coatings, with slightly higher values for the indicated photocatalytic and antimicrobial NS product (Figure 6a–c). The test was validated by considering the results obtained for the paper control, in which all specimens were rated 4 out of 4 (heavy growth, exceeding 60% of the contaminated surface) after the third week of testing.

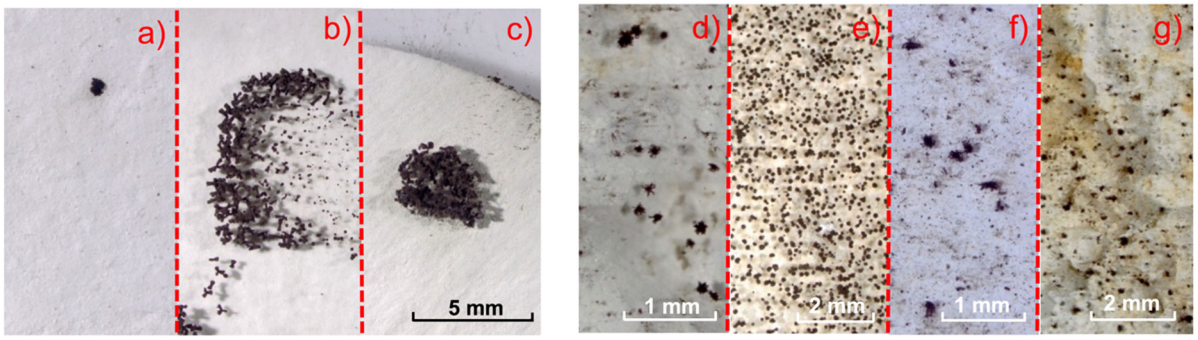

Figure 6. Traces of *A. niger* growth on the unaged multifunctional protective products: (**a**) HW, (**b**) NS, and (**c**) AQ after four weeks of testing. Mold growth observed with NS applied on ETICS: (**d**) S1 and (**e**) S2; (**f**) Mold growth observed with HW applied on ETICS S4; (**g**) ETICS S3 without protective coating.

The results of the average rate of mold development on ETICS after the complete accelerated aging procedure are presented in Figure 7. For the acrylic-finished ETICS S1 and S3 (with EPS and MW insulation, respectively), the application of NS led to an increase in mold development, with moderate mold growth: 30 to 60% of contaminated surface (Figure 6d). Conversely, the application of protective products HW (hydrophobic and biocidal emulsion) and AQ (hydrophobic, self-cleaning and biocidal coating) in ETICS S1 and S3 slightly increased the mold resistance of the system after aging, with only traces of mold growth (<10% of the contaminated surface). In the case of ETICS S3, the surface of this system gained a considerable yellowish tone after accelerated aging (Figure 6f), regardless of the application of protective coatings, mainly due to the use of mineral wool (i.e., thin yellow microfiber) as thermal insulation layer, which was possible partially leached to the drying surface after the HT cycles (e.g., [13]).

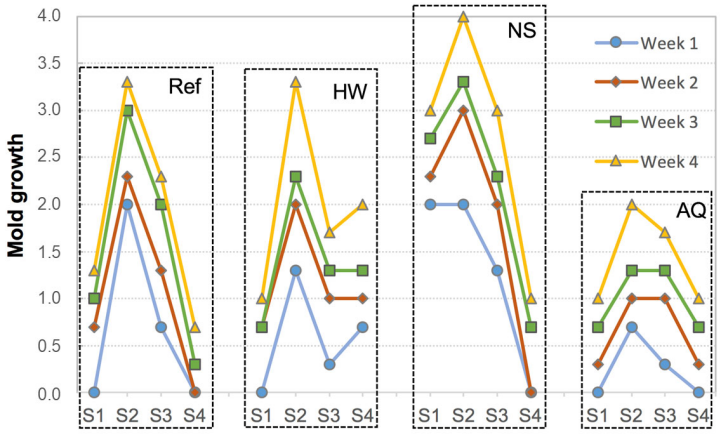

Figure 7. Average results of mold development up to 4 weeks of the untreated (Ref) and treated (HW, NS, and AQ) systems S1–S4. Rating scale: 0—no growth; 1—traces of growth; 2—light growth; 3—moderate growth; 4—heavy growth.

Heavy mold growth (>60% of contaminated surface) was observed with the application of NS (Figure 6e) on the NHL-finished S2 ETICS. In contrast, product AQ slightly increased the resistance to mold development (light growth with 10% to 30% of contaminated surface) in this system after aging. Results showed that the application of HW did not enhance the mold growth resistance of system S2.

Finally, the application of multifunctional products in silicate-finished ETICS S4 contributed to a decrease in mold resistance after aging. In this case, the highest mold development was observed with the application of the siloxane-based HW (Figure 6g), indicating a possible incompatibility between the silicate-based surface and this product.

Although product NS is formulated with remarkable amount of TiO_2 nanoparticles, which might decompose biological macromolecules (DNA) and thus inhibit biological growth [60], as observed in previous studies [61–63], the highest mold growth was generally observed with the application of this product, mainly after artificial aging, with heavy growth in the ETICS with acrylic- (S1 and S3) and NHL-based coating (S2). Conversely, the application of the AQ product slightly increased the resistance to mold growth in ETICSs S1, S2, and S3. Finally, the application of HW did not affect the mold growth resistance of the systems, and in some cases, even induced an increase in bio-susceptibility, as seen with ETICS S4.

3.4. Chemical and Morphological Analyses

3.4.1. SEM-EDS

Results showed that the silicate-based NS protective products formed a thin coating (10–50 µm) when applied to all systems. However, after drying and complete polymerization, the product tended to shrink when applied on the acrylate-finished system (S1 and S3), with a diffuse cracking and a partial detachment of the resulting plate-like clusters [64] (Figure 8a). EDS spectra confirmed a notable amount of titanium, attributed to the photocatalytic TiO_2 nanoparticles (Figure 8c).

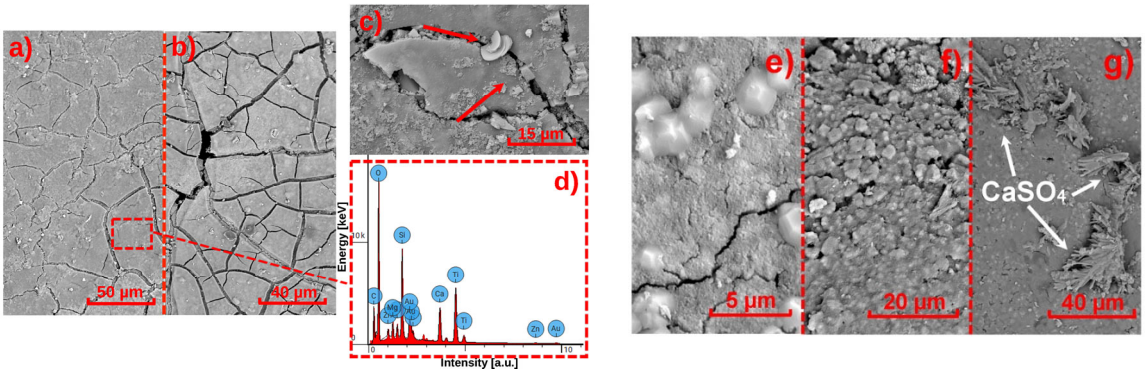

Figure 8. SEM microphotographs of NS product applied on ETICS S1 (**a**) before aging and (**b**) after HT cycles; (**c**) neoformation products (arrows) after SO_2 cycles; (**d**) software-generated EDS elemental spectra of a spot of (**b**); NS product applied on system S2 (**e**) before aging, (**f**) after HT cycles and (**g**) after SO_2 cycles, with acicular gypsum neoformation (arrows).

Cracking generally increased along the aging protocol, mainly after hygrothermal cycles (Figure 8b), with further micro-detachment, dirtiness, and neoformation products observed both after UV and SO_2 cycles (Figure 8d). This trend can be attributed to a combined leaching of the finishing and basecoat of the systems, as well as $CaCO_3$ dissolution-reprecipitation processes [13].

The NS product had a heterogeneous distribution and thus possible lack of compatibility when applied on the NHL-finished S2 system (Figure 8e). The product formed a heterogeneously distributed coating with clusters and suffered an almost complete removal during the hygrothermal cycles (Figure 8f). After the SO_2 cycles, the acicular formation is consistent with gypsum-based clusters (Figure 8g) [65–67], possibly obtained by sulfation, i.e., combination of sulfur dioxide from the pollutant chamber, and the $Ca(OH)_2$ and $CaCO_3$ neoformation [68] after hygrothermal aging. When applied to silicate-finished S4 ETICS, the NS product demonstrated poor physical-chemical compatibility with the substrate, characterized by heterogeneous distribution and material detachment, which consistently increased after artificial aging.

As observed in previous works [69], the high reactivity of the NS silicate binder in an alkaline environment provided by the aqueous medium and the NHL of the substrate (ETICS S2 and S4), and the presence of a relevant amount of $CaCO_3$ can favor the development of shorter linear chains of tetrahedral silica and linear silicate structure, forming colloidal silica gel with plate-like shape [70]. Cracks and surface abnormalities have also been previously reported as a result of a lack of compatibility between protective coatings and the applied substrates [71].

The silane/siloxane emulsion hydrophobic HW product formed a highly compact and homogeneous coating on the acrylate-finished ETICS (S1 and S3) (Figure 9a). Nevertheless, partial decohesion and material loss, and even neoformation products (i.e., calcium carbonate and gypsum) at the surface (Figure 9b), can be noted after the hygrothermal

cycles. A relatively homogeneous and durable HW treatment was observed in the case of the silicate-finished ETICS S4, which can indicate proper compatibility between the product and this rather durable system [15]. Conversely, the application of HW on the NHL-finished S2 system led to a heterogeneous coating, which was seriously damaged after hygrothermal cycles (severe loss of material) (Figure 9c), and again with the formation of carbonate- and sulfate-based clusters after aging cycles with SO_2 (Figure 9d).

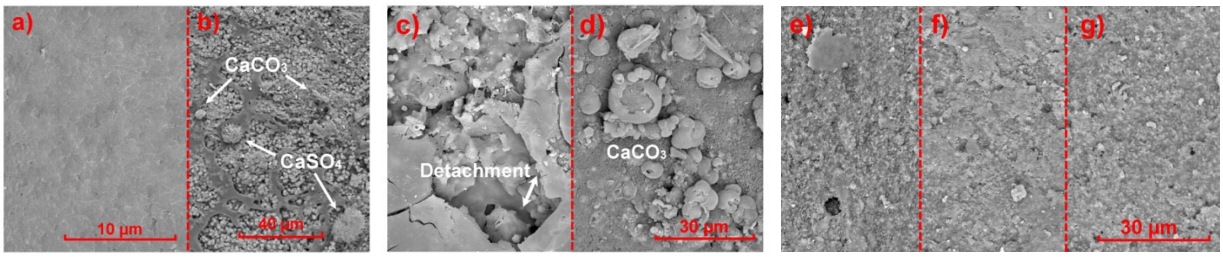

Figure 9. SEM microphotographs of HW product applied on ETICS: S1 (**a**) before aging and (**b**) after SO_2 cycles; S2 (**c**) after HT cycles and (**d**) after SO_2 cycles; AQ product applied on ETICS: (**e**) S1 after SO_2 cycles; (**f**) S2 after SO_2 cycles; (**g**) S4 after HT cycles.

The application of AQ also resulted in a homogeneous coating, with some porosity at the microscale. The coating exhibited high resistance to various aging cycles across all systems (Figure 9e,f) [40,51], possibly due to its enhanced thickness compared to other products. The hygrothermal aging cycles were confirmed to be the most invasive aging procedure, leading to the washing and thus micro-abrasion of the surface, mainly in the case of the NHL-finished S4 system (Figure 9g).

3.4.2. DRIFT

The DRIFT spectra of the finishing coating of ETICS S1, S2, and S4 (untreated), used as reference (Figure 10), showed generally considerable amounts of cement-based or lime-based compounds, as well as additives (inert sands or acrylic resins), in agreement with previous results [13].

After the artificial aging cycles, a higher intensity of the carbonate bands (overlapped $\nu CO_3^{2-}/\delta_{as}CH_3$ mode at ~1400 cm^{-1}; ωCO_3^{2-} mode at 876 cm^{-1}) was observed for ETICS S1 (Figure 10a) and ETICS S2 (Figure 10b,c) after UV cycles, when compared to the unaged ETICS, confirming the presence of leached clusters and additives on the aged substrate. Additionally, an intensity increase in the hydroxyl bands (νOH at ~3300 cm^{-1}, δHOH of adsorbed water at ~1640 cm^{-1}), partially attributed to the presence of $Ca(OH)_2$ [72], confirmed the neoformation of calcium-based products observed in the SEM-EDS analysis (in Section 3.4.1). In the case of ETICS S4, with or without protective products, no significant changes were observed in the spectra after artificial aging with UV and SO_2 cycles, indicating the high stability of the silicate-finished ETICS.

In the DRIFT spectra, a doublet band is observed at ~1795 and ~1740 cm^{-1} that can be assigned to $\nu_s CO_3^{2-}$ modes overlapped with νC=O modes, or to combination bands of the two modes, for the acrylic-finished (ETICS S1) or for polymeric additives (ETICS S2 and S4). A significant change in those bands is observed for ETICS S2, with an inverse evolution to that of carbonates, and therefore can be associated with a possible degradation process.

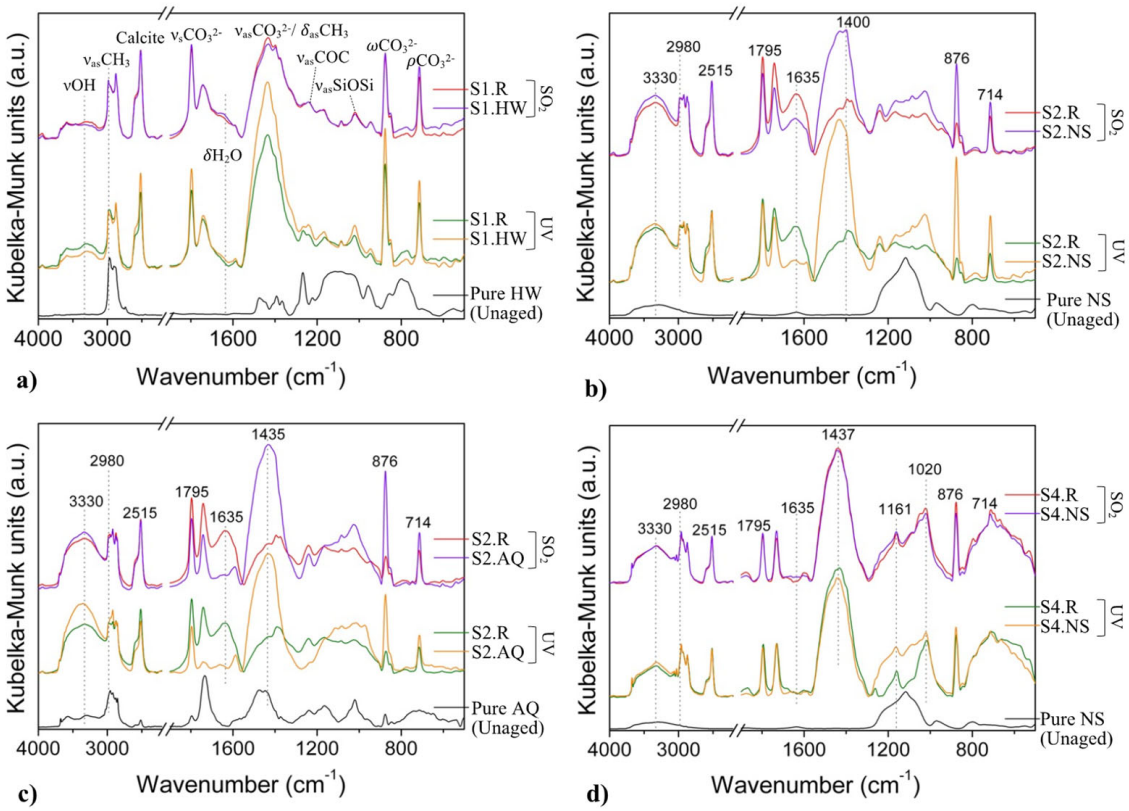

Figure 10. Comparison of DRIFT spectra of the protective coating (unaged) and ETICS without (R) and with protective products (HW, NS, and AQ), after UV and SO_2 aging cycles: (**a**) ETICS S1 with HW; ETICS S2 with (**b**) NS and (**c**) AQ; (**d**) ETICS S4 with NS. The coating spectra are normalized at 2981 cm^{-1}, and the protective coating spectra are normalized at maximum.

Moreover, the decrease in the band at ~3330 cm^{-1} (νOH mode) with an increase in the band at ~1795 cm^{-1} for ETICS S1 after UV irradiation, might arise from the photo-oxidation reaction of –OH, leading to the formation of oxidized products containing C=O chromophores and, thus, a slight yellowish of the surface, in accordance with the results of color change and photocatalytic efficacy (Section 3.2.1) [73]. Finally, a band of the silicate (ν_{as}Si-O-Si mode at ~1020 cm^{-1}) was observed in all ETICS, with the intensity increasing for ETICS S4 (Figure 10d).

When analyzing the ETICS with the protective products, a possible mixture of the signals from the protective product and the reference system materials (finishing and basecoat) can be observed, also due to the method of sample collection, which involves scraping the surface. The bands of the protective products' spectra (pure HW, NS, or AQ) overlap with those of the finishing and basecoat of the ETICS (Figure 10a–d), hindering a clear identification of alterations or degradation of the protective products along the aging protocol. However, the decrease in the δHOH mode (1640 cm^{-1}) can be attributed to the decrease in adsorbed water resulting from the artificial aging cycles of ETICS S2, if accompanied by a reduction in the νOH band, or confirms the possibility of some degradation product formation.

Regarding the acrylate polymers (in the finishing coat of ETICS S1, or the protective product AQ), the presence of monomer acrylic groups can be associated with a νC=C band in the infrared spectrum that can be observed in the same region of the δHOH mode (adsorbed water). Since no changes were observed in the δHOH mode region (at 1640 cm^{-1}) in the spectra of ETICS S1, degradation throughout the aging processes can be excluded, confirming the high durability of the ETICS S1 acrylate coating. In the case of

ETICS S2, the band in the region of the δHOH mode decreased significantly, and the νOH band region increased with artificial aging. Following previous work [14], no partial repair or degradation reversion of the polymer paint was observed, particularly after exposure to UV radiation. The decrease in the relative intensity of the δHOH band may be attributed to a drying process or, more likely, to a chemical reaction between water and a coating component, which increases the number of OH groups and consequently enhances the relative intensity of the νOH band.

Concerning ETICS S4, a relative intensity increase in the band at 1161 cm^{-1} is observed in the sample after UV cycles, which may be due to the presence of the protective product, resulting in an overlap of the finishing coat and protective product bands.

4. Discussion

The photocatalytic and antimicrobial NS treatment (ethyl silicate-based with TiO_2) produced a thin coating with extensive microcracking, which was considered to have poor compatibility with the NHL (S2) and silicate-finished (S4) ETICS. In these systems, the distribution of the coating components was heterogeneous, with cluster-like deposition. Although the formulation included hydrophobic ethyl silicate, the improvement in water repellency was negligible. Hygrothermal aging significantly affected this coating, resulting in partial detachment or surface yellowing. However, the product possibly filled the nano- and micro-porosities of the systems [16], thereby reducing water uptake even after aging. Exposure to UV light activated the TiO_2 particles within the product, resulting in a slightly more hydrophilic surface, which can also favor water vapor permeability and thus evaporation [51].

Although the SO_2 cycles did not seriously affect the coating, with a grayish tone which is only slightly visible to the naked eye, the reduced durability of NS can affect the self-cleaning features over time, with a partial release of TiO_2 nanoparticles during the aging cycles [50,74], followed by a reduction in the photoactivity after exposure to UV radiation and condensation cycles [75]. Investigating the degradation of TiO_2-modified paints under low-radiation conditions, a study observed a rather opposite effect, as microcracks arising from this type of exposure enhanced photocatalytic performance due to a larger exposure area [76]. Therefore, the importance of analyzing different weathering agents is straightforward.

Furthermore, the presence of microcracks influenced the bioreceptivity of the coating, providing potential anchoring points for mold growth and, thus, compromising the expected antimicrobial attribute of the surface [77]. The increase in the drying index after hygrothermal aging can further aggravate this matter, because if drying is not fast enough, the presence of moisture for more extended periods favors biological growth in ETICS [4]. Taken together, the limited stability, durability, and weak compatibility make it unsuitable for long-term use on the studied systems.

The silane/siloxane HW emulsion created a compact, water-repellent coating that was durable and compatible with acrylic-finished S1 and S3 ETICS. In contrast, its distribution was heterogeneous when applied to the NHL-finished S2 system and showed no substantial benefit on the silicate-finished ETICS (S4). However, partial photodegradation of the coatings was observed during UV irradiation [78]. Additionally, the aging of this product can affect the drying rate, especially in the case of highly rough, acrylic-finished surfaces (e.g., S3), where poor self-cleaning properties were observed both before and after aging. HW is therefore suitable for acrylic ETICS, but its application to lime- and silicate-based systems is not recommended.

The acrylic AQ dispersion formed a thicker, more microporous coating than the other products. Its chemical affinity to acrylic ETICS enhanced the compatibility and durability

of the hydrophobic features in S1 and S3, whereas a slight improvement was observed in lime- and silicate-based systems (S2 and S4). The coexistence of hydrophobic acrylic components with hydrophilic TiO_2 resulted in a competitive effect [79], reducing overall water repellency. Additionally, UV further increased surface hydrophilicity due to the activation of photocatalytic additives. Indeed, hydrophobicity is reported to be dependent on the TiO_2 loads within the development of protective coatings [80], requiring fine-tuning to achieve the desired performance.

Compared to NS, the self-cleaning effect of AQ was less pronounced; however, the coating exhibited superior resistance to hygrothermal, UV, and SO_2 aging, particularly when used on acrylic-finished ETICS. Poor results were observed when applied to silicate-finished ETICS S4, possibly due to the lack of a coupling agent (e.g., silane) in the acrylic polymer, which could have increased the physical-chemical compatibility between the organic and inorganic phases [81]. Furthermore, the acrylic AQ coating slowed down the drying rate, compared to the NS and (ethyl silicate) HW products.

Overall, the results indicate apparent differences in performance depending on both the protective product and the ETICS finish. NS provided initial self-cleaning capabilities but failed in terms of durability and compatibility. HW was effective only on acrylic systems, and AQ also combined good durability with moderate self-cleaning in acrylic ETICS, albeit at the expense of drying time. Analogously, in another study, hydrophobic products were also identified as having differing effectiveness and durability when applied to limestone or cementitious mortars [20], thereby underscoring the importance of an integrated assessment.

When selecting between hydrophobic and photocatalytic properties for ETICS, the trade-offs must be weighed. Hydrophobicity reduces water uptake and, thus, can prevent moisture degradation, but it can also limit drying and self-cleaning. Photocatalysis can support surface whitening and pollutant degradation by leveraging increased hydrophilicity; however, this effect is not sustained if low durability is identified, as in the case of NS. For this reason, the selected treatments must be case-oriented, considering the product quality, substrate compatibility, and environmental conditions. Indeed, other research indicates that exposure conditions significantly impact on maintenance needs for ETICS [82].

Although the performance of ETICS has already been investigated in other European contexts, material formulations, construction practices, and aging methodology vary significantly, and these factors strongly influence the durability and compatibility of surface treatments. In addition, most earlier works considered individual parameters, whereas the present study employs a comprehensive set of artificial aging cycles, allowing for a systematic comparison of multifunctional products. This approach provides data that are directly relevant to local building practice and expands the understanding of ETICS performance under different climates.

5. Conclusions

This study evaluated the performance of three commercial multifunctional protective coatings applied to thermal insulating composite systems (ETICS) surfaces, focusing on their effects on moisture transport, photocatalytic activity, color stability, and mold growth before and after accelerated aging. Thus, the research aimed to provide a comprehensive overview of long-term performance and address pressing challenges in building façades. The results underline that the long-term effectiveness of protective treatments is strongly influenced by their chemical compatibility with the underlying ETICS finishes.

Through surface multifunctionality, including water resistance features, different lines of behavior were observed for the four types of ETICS throughout the accelerated aging procedure, which are directly related to the long-term performance of the whole system.

The relevance of the interconnection between moisture transfer, biological colonization, and photocatalytic activity was especially evident for the ethyl-silicate-based coating with TiO_2 applied to NHL finishing ETICS. Poor compatibility, resulting in surface microcracks, may have facilitated mold growth, which can also be favored through an increase in the drying index with hygrothermal aging.

The results were indeed found to be highly dependent on the chemical compatibility between the coatings and the ETICS finishes (acrylic, hydraulic lime, or silicate). On silicate substrates, the application of the protective products led to worse moisture transport properties (i.e., higher water absorption and slower drying) and higher biological colonization, due to reduced compatibility and bonding between the silicate substrate and the waterborne organic products (without a coupling agent). Hydrophobic and/or photocatalytic coatings were somewhat effective and durable on acrylic/finished thermal insulating systems due to their chemical compatibility, which also favors extended long-term performance. On the contrary, low durability and low performance were observed when applied to the hydraulic lime-finished thermal insulating systems.

Concerning durability, both ETICS and protective products were primarily affected by hygrothermal aging, resulting in physical-chemical alterations to the polymeric matrix of the multifunctional coatings or changes in the pore size distribution of the systems. Conversely, the UV cycles led to activation of the photocatalytic and hydrophilic additives, slightly favoring the wettability of the substrates.

Regarding the individual commercial products investigated:

- HW (silane/siloxane emulsion) ensured good water repellency and durability on acrylic ETICS, but showed reduced performance on lime- and silicate-based systems and limited self-cleaning;
- NS (ethyl silicate with TiO_2) offered initial photocatalytic and self-cleaning properties, but a negative performance in terms of biocidal effect, durability, and effectiveness over time;
- AQ (acrylic dispersion with TiO_2) combined acceptable durability and moderate self-cleaning on acrylic systems but increased drying resistance and showed weak performance on mineral-based ETICS.

From a practical standpoint, none of the tested coatings is recommended for silicate-based ETICS, while the ethyl silicate—TiO_2 product should generally be avoided. Protective treatments for acrylic-based ETICS showed more promising results, particularly with HW and AQ. However, the study emphasizes that performance cannot be assessed based on a single property; successful solutions must ensure multifunctionality, combining water repellency, drying capacity, and biological resistance, while avoiding incompatibility that could compromise the hygrothermal balance of the system. In some cases, reapplying the original compatible finish may represent the most reliable strategy to safeguard ETICS durability, insulation efficiency, and long-term energy performance.

Author Contributions: Conceptualization, G.B., J.L.P., R.V., A.D., P.F. and I.F.-C.; methodology, G.B., J.L.P., R.V., A.D., P.F. and I.F.-C.; validation, G.B., J.L.P., A.R.G., A.D., P.F., R.V. and I.F.-C.; formal analysis, G.B., J.L.P., A.R.G., A.D., P.F., R.V. and I.F.-C.; investigation, G.B., J.L.P., A.D. and A.R.G.; data curation, G.B., J.L.P., J.D.B. and A.R.G.; writing—original draft preparation, G.B., J.L.P., J.D.B. and A.R.G.; writing—review and editing, A.R.G., R.V., A.D., P.F. and I.F.-C.; funding acquisition, I.F.-C. and R.V. All authors have read and agreed to the published version of the manuscript.

Funding: This research was funded by FUNDAÇÃO PARA A CIÊNCIA E A TECNOLOGIA (FCT), within the research project WGB_Shield (PTDC/ECI-EGC/30681/2017). The authors acknowledge the financial support of the FCT through the project UIDB/04625/2025 of the research unit CERIS and UIDB/04028/2020 of CERENA. The third author acknowledges the FCT grant number 2023.05316.BD (DOI: https://doi.org/10.54499/2023.05316.BD).

Data Availability Statement: The raw data supporting the conclusions of this article will be made available by the authors on request.

Acknowledgments: In Memoriam of Dr. Lina Nunes, who actively collaborated in this and several previous projects.

Conflicts of Interest: The authors declare no conflicts of interest.

Abbreviations

The following abbreviations are used in this manuscript:

θ	Contact Angle
ΔE	Color Change
a*	Color Coordinate (red-green)
AQ	Hydrophobic, Self-cleaning and Biocidal Coating
b*	Color Coordinate (yellow-blue)
BC	Base Coat
Cc	Capillary Water Absorption Coefficient
DI	Drying Index
DRIFT	Diffuse Reflectance Infrared Fourier Transform
EDS	Energy Dispersive Spectroscopy
EIFS	Exterior Insulation Finishing System
EPS	Expanded Polystyrene
ETA	European Technical Approval
ETICS	External Thermal Insulation Composite Systems
EWI	Exterior Wall Insulation Systems
FC	Finishing Coat
HT	Hygrothermal Cycles
HW	Hydrophobic and Biocidal Coating
ICB	Insulation Cork Board
L*	Lightness
MC	Multifunctional Coatings
MW	Mineral Wool
NHL	Natural Hydraulic Lime
NS	Photocatalytic Self-Cleaning and Antimicrobial Coating
Ref	Without Protective Treatment
RH	Relative Humidity
RhB	Rhodamine B
S1	System 1
S2	System 2
S3	System 3
S4	System 4
SCI	Specular Component Included
SEM	Scanning Electron Microscope
SO_2	Air Pollutant Cycles
T	Temperature
UV	Ultraviolet Radiation Cycles

References

1. Malanho, S.; Veiga, M.R. Bond strength between layers of ETICS—Influence of the characteristics of mortars and insulation materials. *J. Build. Eng.* **2020**, *28*, 101021. [CrossRef]
2. Amaro, B.; Saraiva, D.; De Brito, J.; Flores-Colen, I. Inspection and diagnosis system of ETICS on walls. *Constr. Build. Mater.* **2013**, *47*, 1257–1267. [CrossRef]
3. *EAD 040083-00-0404*; External Thermal Insulation Composite Systems (ETICS) with Rendering. EOTA (European Organisation for Technical Approvals): Brussels, Belgium, 2020; pp. 1–88.
4. Barreira, E.; de Freitas, V.P. Experimental study of the hygrothermal behaviour of External Thermal Insulation Composite Systems (ETICS). *Build. Environ.* **2013**, *63*, 31–39. [CrossRef]
5. Xu, H.; Wang, H.; Huo, Q.; Qin, Y.; Zhou, H. Comparative study of Chinese, European and ISO external thermal insulation composite system (ETICS) standards and technical recommendations. *J. Build. Eng.* **2023**, *68*, 105687. [CrossRef]
6. Malanho, S.; Veiga, R.; Farinha, C. Global Performance of Sustainable Thermal Insulating Systems with Cork for Building Facades. *Buildings* **2021**, *11*, 83. [CrossRef]
7. Parracha, J.L.; Borsoi, G.; Flores-Colen, I.; Veiga, R.; Nunes, L.; Dionísio, A.; Gomes, M.G.; Faria, P. Performance parameters of ETICS: Correlating water resistance, bio-susceptibility and surface properties. *Constr. Build. Mater.* **2021**, *272*, 121956. [CrossRef]
8. Zhou, X.; Kubilay, A.; Derome, D.; Carmeliet, J. Comparison of wind-driven rain load on building facades in the urban environment and open field: A case study on two buildings in Zurich, Switzerland. *Build. Environ.* **2023**, *233*, 110038. [CrossRef]
9. Bauer, E.; Souza, A.L.R. Failure patterns associated with facade zones and anomalies in the initiation and propagation of degradation. *Constr. Build. Mater.* **2022**, *347*, 128563. [CrossRef]
10. Ren, H.; Koshy, P.; Chen, W.F.; Qi, S.; Sorrell, C.C. Photocatalytic materials and technologies for air purification. *J. Hazard. Mater.* **2017**, *325*, 340–366. [CrossRef] [PubMed]
11. De la Rosa, J.M.; Miller, A.Z.; Pozo-Antonio, J.S.; González-Pérez, J.A.; Jiménez-Morillo, N.T.; Dionisio, A. Assessing the effects of UVA photocatalysis on soot-coated TiO_2-containing mortars. *Sci. Total Environ.* **2017**, *605–606*, 147–157. [CrossRef]
12. Amaro, B.; Saraiva, D.; De Brito, J.; Flores-Colen, I. Statistical survey of the pathology, diagnosis and rehabilitation of ETICS in walls. *J. Civ. Eng. Manag.* **2014**, *20*, 511–526. [CrossRef]
13. Parracha, J.L.; Borsoi, G.; Veiga, R.; Flores-Colen, I.; Nunes, L.; Garcia, A.R.; Ilharco, M.; Dionísio, A.; Faria, P. Effects of hygrothermal, UV and SO_2 accelerated ageing on the durability of ETICS in urban environments. *Build. Environ.* **2021**, *204*, 108151. [CrossRef]
14. Veigas, C.A.; Borsoi, G.; Moreira, L.M.; Parracha, J.L.; Nunes, L.; Malanho, S.; Veiga, R.; Flores-Colen, I. Diversity and distribution of microbial communities on the surface of External Thermal Insulation Composite Systems (ETICS) facades in residential buildings. *Int. Biodeterior. Biodegrad.* **2023**, *184*, 105658. [CrossRef]
15. Vega-Garcia, P.; Lok, C.S.C.; Marhoon, A.; Schwerd, R.; Johann, S.; Helmreich, B. Modelling the environmental fate and behavior of biocides used in façades covered with mortars and plasters and their transformation products. *Build. Environ.* **2022**, *216*, 108991. [CrossRef]
16. Silva, A.S.; Borsoi, G.; Parracha, J.L.; Flores-Colen, I.; Veiga, R.; Faria, P.; Dionísio, A. Evaluating the effectiveness of self-cleaning products applied on external thermal insulation composite systems (ETICS). *J. Coat. Technol. Res.* **2022**, *19*, 1437–1448. [CrossRef]
17. Wang, L.; Zhang, J.; Wang, F.; Liu, Z.; Su, W.; Chen, Z.; Jiang, J. Investigation on the effects of polyaniline/lignin composites on the performance of waterborne polyurethane coating for protecting cement-based materials. *J. Build. Eng.* **2023**, *64*, 105665. [CrossRef]
18. Heib, F.; Hempelmann, R.; Munief, W.M.; Ingebrandt, S.; Fug, F.; Possart, W.; Groß, K.; Schmitt, M. High-precision drop shape analysis (HPDSA) of quasistatic contact angles on silanized silicon wafers with different surface topographies during inclining-plate measurements: Influence of the surface roughness on the contact line dynamics. *Appl. Surf. Sci.* **2015**, *342*, 11–25. [CrossRef]
19. Chen, Y.; Wang, R.; Wang, H.; Hu, F.; Jin, P. Study on PVA-siloxane mixed emulsion coatings for hydrophobic cement mortar. *Prog. Org. Coat.* **2020**, *147*, 105775. [CrossRef]
20. Borsoi, G.; Esteves, C.; Flores-Colen, I.; Veiga, R. Effect of hygrothermal aging on hydrophobic treatments applied to building exterior claddings. *Coatings* **2020**, *10*, 363. [CrossRef]
21. van Duijkeren, E.; Schink, A.K.; Roberts, M.C.; Wang, Y.; Schwarz, S. Mechanisms of Bacterial Resistance to Antimicrobial Agents. *Microbiol. Spectr.* **2018**, *6*, 2. [CrossRef]
22. Castro-Hoyos, A.M.; Rojas Manzano, M.A.; Maury-Ramírez, A. Challenges and Opportunities of Using Titanium Dioxide Photocatalysis on Cement-Based Materials. *Coatings* **2022**, *12*, 968. [CrossRef]
23. Riaz, S.; Park, S.J. An overview of TiO_2-based photocatalytic membrane reactors for water and wastewater treatments. *J. Ind. Eng. Chem.* **2020**, *84*, 23–41. [CrossRef]
24. Hot, J.; Dasque, A.; Topalov, J.; Mazars, V.; Ringot, E. Titanium valorization: From chemical milling baths to air depollution applications. *J. Clean. Prod.* **2020**, *249*, 119344. [CrossRef]

25. Padmanabhan, N.T.; Thomas, R.M.; John, H. Antibacterial self-cleaning binary and ternary hybrid photocatalysts of titanium dioxide with silver and graphene. *J. Environ. Chem. Eng.* **2022**, *10*, 107275. [CrossRef]
26. La Russa, M.F.; Ruffolo, S.A.; Rovella, N.; Belfiore, C.M.; Palermo, A.M.; Guzzi, M.T.; Crisci, G.M. Multifunctional TiO_2 coatings for Cultural Heritage. *Prog. Org. Coat.* **2012**, *74*, 186–191. [CrossRef]
27. Celia, E.; Darmanin, T.; Taffin de Givenchy, E.; Amigoni, S.; Guittard, F. Recent advances in designing superhydrophobic surfaces. *J. Colloid. Interface Sci.* **2013**, *402*, 1–18. [CrossRef]
28. Nath, R.K.; Zain, M.F.M.; Jamil, M. An environment-friendly solution for indoor air purification by using renewable photocatalysts in concrete: A review. *Renew. Sustain. Energy Rev.* **2016**, *62*, 1184–1194. [CrossRef]
29. Higashimoto, S. Titanium-dioxide-based visible-light-sensitive photocatalysis: Mechanistic insight and applications. *Catalysts* **2019**, *9*, 201. [CrossRef]
30. Munafò, P.; Goffredo, G.B.; Quagliarini, E. TiO_2-based nanocoatings for preserving architectural stone surfaces: An overview. *Constr. Build. Mater.* **2015**, *84*, 201–218. [CrossRef]
31. Vega-Garcia, P.; Schwerd, R.; Scherer, C.; Schwitalla, C.; Johann, S.; Rommel, S.H.; Helmreich, B. Influence of façade orientation on the leaching of biocides from building façades covered with mortars and plasters. *Sci. Total Environ.* **2020**, *734*, 139465. [CrossRef]
32. European Union. Regulation (EU) No 528/2012 of the European Parliament and of the Council of 22 May 2012 concerning the Making Available on the Market and Use of Biocidal Products. *Off. J. Eur. Union* **2022**, *167*, 1–123.
33. Schoknechta, U.; Sommerfelda, T.; Borhob, N.; Bagdab, E. Interlaboratory comparison for a laboratory leaching test procedure with façade coatings. *Prog. Org. Coat.* **2013**, *76*, 351–359. [CrossRef]
34. Bollmann, U.E.; Minelgaite, G.; Schlüsener, M.; Ternes, T.; Vollertsen, J.; Bester, K. Leaching of Terbutryn and Its Photodegradation Products from Artificial Walls under Natural Weather Conditions. *Environ. Sci. Technol.* **2016**, *50*, 4289–4295. [CrossRef] [PubMed]
35. La Russa, M.F.; Rovella, N.; Alvarez De Buergo, M.; Belfiore, C.M.; Pezzino, A.; Crisci, G.M.; Ruffolo, S.A. Nano-TiO_2 coatings for cultural heritage protection: The role of the binder on hydrophobic and self-cleaning efficacy. *Prog. Org. Coat.* **2016**, *91*, 1–8. [CrossRef]
36. Diamanti, M.V.; Luongo, N.; Massari, S.; Lupica Spagnolo, S.; Daniotti, B.; Pedeferri, M.P. Durability of self-cleaning cement-based materials. *Constr. Build. Mater.* **2021**, *280*, 122441. [CrossRef]
37. Bersch, J.D.; Flores-Colen, I.; Masuero, A.B.; Dal Molin, D.C.C. Photocatalytic TiO_2-Based Coatings for Mortars on Facades: A Review of Efficiency, Durability, and Sustainability. *Buildings* **2023**, *13*, 186. [CrossRef]
38. Goffredo, G.B.; Terlizzi, V.; Munafò, P. Multifunctional TiO_2-based hybrid coatings on limestone: Initial performances and durability over time. *J. Build. Eng.* **2017**, *14*, 134–149. [CrossRef]
39. *EN 16322:2013*; Conservation of Cultural Heritage—Test Methods—Determination of Drying Properties. CEN: Brussels, Belgium, 2013.
40. Parracha, J.L.; Borsoi, G.; Veiga, R.; Flores-Colen, I.; Nunes, L.; Viegas, C.A.; Moreira, L.M.; Dionísio, A.; Glória Gomes, M.; Faria, P. Durability assessment of external thermal insulation composite systems in urban and maritime environments. *Sci. Tot. Environ.* **2022**, *849*, 157828. [CrossRef]
41. *UNI 11259*; Determination of the Photocatalytic Activity of Hydraulic Binders—Rhodamine Method (in Italian). UNI: Milan, Italy, 2008.
42. Krishnan, P.; Zhang, M.H.; Yu, L.; Feng, H. Photocatalytic degradation of particulate pollutants and self-cleaning performance of TiO_2-containing silicate coating and mortar. *Constr. Build. Mater.* **2013**, *44*, 309–316. [CrossRef]
43. *ASTM-D2244*; Standard Practice for Calculation of Color Tolerances and Color Differences from Instrumentally Measured Color Coordinates. ASTM International: West Conshohocken, PA, USA, 2022.
44. Munafò, P.; Quagliarini, E.; Goffredo, G.B.; Bondioli, F.; Licciulli, A. Durability of nano-engineered TiO_2 self-cleaning treatments on limestone. *Constr. Build. Mater.* **2014**, *65*, 218–231. [CrossRef]
45. *ASTM C1338-19*; Standard Test Method for Determining Fungi Resistance of Insulation Materials and Facings. ASTM: West Conshohocken, PA, USA, 2019.
46. *ASTM D5590-17*; Standard Test Method for Determining the Resistance of Paint Films and Related Coatings to Fungal Defacement by Accelerated Four-Week Agar Plate Assay. ASTM: West Conshohocken, PA, USA, 2017.
47. Parracha, J.L.; Borsoi, G.; Flores-Colen, I.; Veiga, R.; Nunes, L. Impact of natural and artificial ageing on the properties of multilayer external wall thermal insulation systems. *Constr. Build. Mater.* **2022**, *317*, 125834. [CrossRef]
48. *ISO 16474-3*; Paints and Varnishes—Methods of Exposure to Laboratory Light Sources—Part 3, Fluorescent UV Lamps. ISO: Geneva, Switzerland, 2013.
49. Diamanti, M.V.; Paolini, R.; Rossini, M.; Aslan, A.B.; Zinzi, M.; Poli, T.; Pedeferri, M.P. Long term self-cleaning and photocatalytic performance of anatase added mortars exposed to the urban environment. *Constr. Build. Mater.* **2015**, *96*, 270–278. [CrossRef]
50. Graziani, L.; Quagliarini, E.; Bondioli, F.; D'Orazio, M. Durability of self-cleaning TiO_2 coatings on fired clay brick façades: Effects of UV exposure and wet & dry cycles. *Build. Environ.* **2014**, *71*, 193–203. [CrossRef]

51. Roncon, R.; Borsoi, G.; Parracha, J.L.; Flores-Colen, I.; Veiga, R.; Nunes, L. Impact of water-repellent products on the moisture transport properties and mould susceptibility of external thermal insulation composite systems. *Coatings* **2021**, *11*, 554. [CrossRef]
52. Ghaee, A.; Ghadimi, A.; Sadatnia, B.; Ismail, A.F.; Mansourpour, Z.; Khosravi, M. Synthesis and characterization of poly(vinylidene fluoride) membrane containing hydrophobic silica nanoparticles for CO_2 absorption from CO_2/N_2 using membrane contactor. *Chem. Eng. Res. Des.* **2017**, *120*, 47–57. [CrossRef]
53. Quéré, D. Non-sticking drops. *Rep. Prog. Phys.* **2005**, *68*, 2495–2532. [CrossRef]
54. Sadat-Shojai, M.; Ershad-Langroudi, A. Polymeric coatings for protection of historic monuments: Opportunities and challenges. *J. Appl. Polym. Sci.* **2009**, *112*, 2535–2551. [CrossRef]
55. Feltes, J.; Borsoi, G.; Caiado, P.; Dionísio, A.; Parracha, J.; Flores-Colen, I. Graffiti removal on external thermal insulation composite systems through chemical-mechanical methods: A feasible protocol? *J. Build. Eng.* **2023**, *66*, 105872. [CrossRef]
56. Lu, T.; Solis-Ramos, E.; Yi, Y.; Kumosa, M. UV degradation model for polymers and polymer matrix composites. *Polym. Degrad. Stab.* **2018**, *154*, 203–210. [CrossRef]
57. Gil, B.C.; Borsoi, G.; Parracha, J.L.; Dionísio, A.; Veiga, R.; Flores-Colen, I. Effectiveness and durability of anti-graffiti products applied on ETICS: Towards a compatible and sustainable graffiti removal protocol. *Environ. Sci. Pollut. Res.* **2023**, *30*, 65160–65176. [CrossRef] [PubMed]
58. Folli, A.; Pade, C.; Hansen, T.B.; De Marco, T.; MacPhee, D.E. TiO_2 photocatalysis in cementitious systems: Insights into self-cleaning and depollution chemistry. *Cem. Concr. Res.* **2012**, *42*, 539–548. [CrossRef]
59. Calia, A.; Lettieri, M.; Masieri, M. Durability assessment of nanostructured TiO_2 coatings applied on limestones to enhance building surface with self-cleaning ability. *Build. Environ.* **2016**, *110*, 1–10. [CrossRef]
60. Solovyeva, M.; Selishchev, D.; Cherepanova, S.; Stepanov, G.; Zhuravlev, E.; Richter, V.; Kozlov, D. Self-Cleaning Photoactive Cotton Fabric Modified with Nanocrystalline TiO_2 for Efficient Degradation of Volatile Organic Compounds and DNA Contaminants. *Chem. Eng. J.* **2020**, *388*, 124167. [CrossRef]
61. Guo, M.-Z.; Ling, T.-C.; Poon, C.-S. Nano-TiO_2-based architectural mortar for NO removal and bacteria inactivation: Influence of coating and weathering conditions. *Cem. Concr. Compos.* **2013**, *36*, 101–108. [CrossRef]
62. Maury-Ramirez, A.; De Muynck, W.; Stevens, R.; Demeestere, K.; De Belie, N. Titanium dioxide based strategies to prevent algal fouling on cementitious materials. *Cem. Concr. Compos.* **2013**, *36*, 93–100. [CrossRef]
63. Hegyi, A.; Grebenişan, E.; Lăzărescu, A.; Stoian, V.; Szilagyi, H. Influence of TiO_2 Nanoparticles on the Resistance of Cementitious Composite Materials to the Action of Fungal Species. *Materials.* **2021**, *14*, 4442. [CrossRef] [PubMed]
64. Borsoi, G.; Veiga, R.; Santos Silva, A. Effect of nanostructured lime-based and silica-based products on the consolidation of historical renders. In Proceedings of the 3rd Historic Mortars Conference, Glasgow, Scotland, 11–14 September 2013.
65. Kim, J.; Kim, D.; Yun, T.S. Containment of sulfate in leachate as gypsum ($CaSO_4 \cdot 2H_2O$) mineral formation in bio-cemented sand via enzyme-induced carbonate precipitation. *Sci. Rep.* **2023**, *13*, 10938. [CrossRef]
66. Kistanova, N.S.; Chashchukhina, A.D.; Kudryashova, O.S.; Khayrulina, E.A. Influence of polyacrylamide on the precipitation of gypsum in sodium chloride solutions. *Environ. Earth Sci.* **2023**, *82*, 565. [CrossRef]
67. İnceoğlu, F.; Mermer, N.K.; Kırmızı, V.; Tombaş, G. Influence of cement with different calcium sulfate phases on cementitious tile adhesive mortars: Microstructure and performance aspects. *Int. J. Adhes. Adhes.* **2021**, *104*, 102744. [CrossRef]
68. Biedunkova, O.; Kuznietsov, P.; Gandziure, V. Behaviour of dissolved inorganic salts in the cooling water of a nuclear power plant open recirculation system and formation of water discharge. *R. Soc. Open Sci.* **2024**, *11*, 240492. [CrossRef]
69. Borsoi, G.; Tavares, M.; Veiga, R.; Santos Silva, A. Microstructural characterization of consolidant products for historical renders: An innovative nanostructured lime dispersion and a more traditional ethyl silicate limewater solution. *Microsc. Microanal.* **2012**, *18*, 1181–1189. [CrossRef]
70. Zendri, E.; Biscontin, G.; Nardini, I.; Rialto, S. Characterization and reactivity of silicatic consolidants. *Constr. Build. Mater.* **2007**, *21*, 1098–1106. [CrossRef]
71. Hashim, H.; Dias, L.; Martins, S.; Pires, V.; Costa, M.; Barrulas, P. Optimization of the Application of Commercial Hydrophobic Coatings for Natural Stone Protection and Preservation. *Heritage* **2024**, *7*, 3495–3510. [CrossRef]
72. Hoyos-Montilla, A.A.; Puertas, F.; Molina Mosquera, J.; Tobón, J.I. Infrared spectra experimental analyses on alkali-activated fly ash-based binders. *Spectrochim. Acta A Mol. Biomol. Spectrosc.* **2022**, *269*, 120698. [CrossRef]
73. Shanti, R.; Hadi, A.N.; Salim, Y.S.; Chee, S.Y.; Ramesh, S.; Ramesha, K. Degradation of ultra-high molecular weight poly(methyl methacrylate-co-butyl acrylate-coacrylic acid) under ultra violet irradiation. *RSC Adv.* **2017**, *7*, 112. [CrossRef]
74. Olabarrieta, J.; Zorita, S.; Peña, I.; Rioja, N.; Monzón, O.; Benguria, P.; Scifo, L. Aging of photocatalytic coatings under a water flow: Long run performance and TiO_2 nanoparticles release. *Appl. Catal. B* **2012**, *123–124*, 182–192. [CrossRef]
75. Carmona-Quiroga, P.M.; Martínez-Ramírez, S.; Viles, H.A. Efficiency and durability of a self-cleaning coating on concrete and stones under both natural and artificial ageing trials. *Appl. Surf. Sci.* **2018**, *433*, 312–320. [CrossRef]
76. Kalinowski, M.; Chilmon, K.; Kuziak, J.; Łukowski, P. Photocatalytically Induced Degradation of Nano-TiO_2-Modified Paint Coatings Under Low-Radiation Conditions. *Coatings* **2025**, *15*, 281. [CrossRef]

77. Sanmartín, P.; Noya-Pintos, D.; Fuentes, E.; Pozo-Antonio, J.S. Cracks in consolidants containing TiO_2 as a habitat for biological colonization: A case of quaternary bioreceptivity. *Mat. Sci. Eng. C* **2021**, *124*, 112058. [CrossRef] [PubMed]
78. Wojciechowski, K.; Skowera, E.; Pietniewicz, E.; Zukowska, G.Z.; Van Der Ven, L.G.J.; Korczagin, I.; Malanowski, P. UV stability of polymeric binder films used in waterborne facade paints. *Prog. Org. Coat.* **2014**, *77*, 298–304. [CrossRef]
79. Fukaya, N.; Ogi, S.; Sotome, H.; Fujimoto, K.J.; Yanai, T.; Bäumer, N.; Fernández, G.; Miyasaka, H.; Yamaguch, S. Impact of Hydrophobic/Hydrophilic Balance on Aggregation Pathways, Morphologies, and Excited-State Dynamics of Amphiphilic Diketopyrrolopyrrole Dyes in Aqueous Media. *J. Am. Chem. Soc.* **2022**, *144*, 22479–22492. [CrossRef]
80. Colangiuli, D.; Calia, A.; Bianco, N. Novel multifunctional coatings with photocatalytic and hydrophobic properties for the preservation of the stone building heritage. *Const. Build. Mat.* **2015**, *93*, 189–196. [CrossRef]
81. Ribeiro, T.; Baleizão, C.; Farinha, J.P. Functional Films from Silica/Polymer Nanoparticles. *Materials* **2014**, *7*, 3881–3900. [CrossRef] [PubMed]
82. Ferreira, C.; Barrelas, J.; Silva, A.; De Brito, J.; Dias, I.S. Impact of Environmental Exposure Conditions on the Maintenance of Facades' Claddings. *Buildings* **2021**, *11*, 138. [CrossRef]